Contribution of local regeneration of glucocorticoids to tissue steroid pools

CONTRIBUTION OF LOCAL REGENERATION OF GLUCOCORTICOIDS TO TISSUE STEROID POOLS

Khan S[1], Livingstone DEW[1,2], Zielinska A[3], Doig CL[4], Cobice DF[1], Esteves CL[1], Man JTY[1], Homer NZM[5], Seckl JR[1], MacKay CL[6], Webster SP[1], Lavery GG[4], Chapman KE[1], Walker BR[1,7], Andrew R[1,4]

[1] Centre for Cardiovascular Science, Queen's Medical Research Institute, University of Edinburgh, 47, Little France Crescent, Edinburgh, EH16 4TJ

[2] Centre for Discovery Brain Science, University of Edinburgh, Hugh Robson Building, 15 George Square, Edinburgh, EH8 9XD, UK.

[3] College of Medical and Dental Sciences, University of Birmingham, Birmingham, B15 2TT, UK

[4] Department of Biosciences, School of Science & Technology, Nottingham Trent University, Clifton Lane, Nottingham, NG11 8NS

[5] Mass Spectrometry Core Laboratory, Edinburgh Clinical Research Facility, Queen's Medical Research Institute, University of Edinburgh, 47, Little France Crescent, Edinburgh, EH16 4TJ

[6] SIRCAMS, School of Chemistry, University of Edinburgh, Joseph Black Building, King's Buildings, West Mains Road, Edinburgh, EH9 3JJ, UK.

[7] Clinical & Translational Research Institute, Newcastle University, International Centre for Life, Central Parkway, Newcastle upon Tyne, NE1 3BZ, UK

Corresponding Author: Professor Ruth Andrew; Ruth.Andrew@ed.ac.uk

Current Addresses

DFC: Biomedical Sciences Research Institute, School of Biomedical Sciences, University of Ulster, Coleraine campus, Cromore Road, Coleraine, Co. Londonderry, BT52 1SA, UK.

d.cobice@ulster.ac.uk

CE: The Roslin Institute, University of Edinburgh, EH25 9RG

Short title: Regeneration of tissue glucocorticoid pools

Keywords: 11β-hydroxysteroid dehydrogenase 1, hexose-6-phosphate dehydrogenase, glucocorticoid, liver, adipose tissue, brain

Word Count: 5526

ABSTRACT:

11β-Hydroxysteroid dehydrogenase 1 (11βHSD1) is a drug target to attenuate adverse effects of chronic glucocorticoid excess. It catalyses intracellular regeneration of active glucocorticoids in tissues including brain, liver and adipose tissue (coupled to hexose-6-phosphate dehydrogenase, H6PDH). 11βHSD1 activity in individual tissues is thought to contribute significantly to glucocorticoid levels at those sites, but its local contribution versus glucocorticoid delivery via the circulation is unknown. Here, we hypothesised that hepatic 11βHSD1 would contribute significantly to the circulating pool. This was studied in mice with Cre-mediated disruption of *Hsd11b1* in liver (*Alac*-Cre) versus adipose tissue (*aP2*-Cre) or whole-body disruption of *H6pdh*. Regeneration of [9,12,12-$^{2}H_3$]-cortisol (d3F) from [9,12,12-$^{2}H_3$]-cortisone (d3E), measuring 11βHSD1 reductase activity was assessed at steady state following infusion of [9,11,12,12-$^{2}H_4$]-cortisol (d4F) in male mice. Concentrations of steroids in plasma and amounts in liver, adipose tissue and brain were measured using mass spectrometry interfaced with matrix assisted laser desorption ionisation or liquid chromatography. Amounts of d3F were higher in liver, compared with brain and adipose tissue. Rates of appearance of d3F were ~6-fold slower in *H6pdh*$^{-/-}$ mice, showing the importance of whole-body 11βHSD1 reductase activity. Disruption of liver 11βHSD1 reduced amounts of d3F in liver (by ~36%), without changes elsewhere. In contrast disruption of 11βHSD1 in adipose tissue reduced rates of appearance of circulating d3F (by ~67%) and also reduced regeneration of d3F in liver and brain (both by ~30%). Thus, the contribution of hepatic 11βHSD1 to circulating glucocorticoid levels and amounts in other tissues is less than that of adipose tissue.

INTRODUCTION

11β-Hydroxysteroid dehydrogenase 1 (11βHSD1) generates active 11-hydroxy glucocorticoids (cortisol (human), corticosterone (rodent and human)) from intrinsically inert 11-keto steroids (cortisone, 11-dehydrocorticosterone (11DHC), respectively)(Anderson and Walker 2013; Chapman, et al. 2013). 11βHSD1 acts in conjunction with hexose-6-phosphate dehydrogenase (H6PDH) which supplies its NADPH co-factor (Lavery, et al. 2006). Chronic glucocorticoid excess causes a spectrum of adverse effects including type 2 diabetes, hypertension, visceral obesity, myopathy, mood disturbances and cognitive deficits and 11βHSD1 has therefore emerged as a drug target to reduce active glucocorticoid levels (Hughes, et al. 2008) in a tissue-specific manner. This can be achieved by inhibiting 11βHSD1 directly or through restricting co-factor availability. Some drug candidates have reached clinical trials (Feig, et al. 2011; Heise, et al. 2014; Rosenstock, et al. 2010; Shah, et al. 2011).

Initial trials investigated the potential of 11βHSD1 inhibitors to improve glycaemic control in patients with type 2 diabetes mellitus, based on pre-clinical studies showing an improved metabolic phenotype in mice with targeted disruption of the *Hsd11b1* gene (Kotelevtsev, et al. 1997; Morton, et al. 2004). Short-term experimental studies of inhibitors in rodents (Hermanowski-Vosatka, et al. 2005; Liu, et al. 2011) and humans (Andrews, et al. 2002; Sandeep, et al. 2005) supported this concept, but did not achieve better endpoints than current therapies (Feig et al. 2011; Heise et al. 2014; Rosenstock et al. 2010; Shah et al. 2011). Brain penetrant 11βHSD1 inhibitors have been evaluated as potential therapies for Alzheimer's disease and other age-related cognitive impairments, (Katz, et al. 2013; Webster, et al. 2007; Yau, et al. 2011; Yau, et al. 2015; Yau, et al. 2007a; Yau, et al. 2001) with candidates

(Webster, et al. 2016) currently in phase II clinical trials (e.g. NCT05657691). This therapeutic concept has evolved from preclinical studies demonstrating beneficial effects upon cognition in aged animals following reductions in whole body levels of glucocorticoids in mice (Yau et al. 2011; Yau et al. 2015; Yau et al. 2007a; Yau et al. 2001). This can be achieved bluntly by removing the adrenal glands which are the major source of endogenous glucocorticoids (Montaron, et al. 2006), with the risk of Addisonian crisis, but also more subtly by reducing 11βHSD1 activity through lifelong genetic disruption (Yau et al. 2011; Yau et al. 2001; Yau, et al. 2007b) or with short-term pharmacological inhibition of 11βHSD1 activity (Sooy, et al. 2010; Sooy, et al. 2015; Webster et al. 2016). The potential of 11βHSD1 inhibitors to improve wound healing is under clinical translation (Ajjan, et al. 2022) and preclinical studies highlight the opportunities for 11βHSD1 inhibitors to enhance tissue repair after myocardial infarction (Mylonas, et al. 2017). Thus, there are many applications of the drug class, each requiring assessment of changes in amounts of active glucocorticoids (and ratios versus inactive steroids) in specific tissue sites.

Recent advances in pharmacodynamic monitoring through mass spectrometry (MS) have allowed tracing of glucocorticoids *in situ* and shown suppression of the ratio of active (cortisol/cortisone)/inert (corticosterone/11-DHC) in response to 11βHSD1 inhibition in brain regions (Cobice, et al. 2017). However, it remains unclear the extent to which 11βHSD1 in individual tissues contributes to the circulating pool of active steroid and how changes in glucocorticoid regeneration in one tissue can influence active steroid levels in another, if at all. In humans, contributions of 11βHSD1 within different tissues to whole body regeneration of active glucocorticoids have been explored by tracer kinetics in conjunction with arteriovenous sampling and biopsy. The reductive activity of 11βHSD1 has been tracked using dilution of the administered tracer [9,11,12,12-$^{2}H_4$]-cortisol (d4F) by [9,11,12,12-$^{2}H_3$]-

cortisol (d3F) which reflects the steroid regenerated by 11β-reduction, via the intermediate [9,12,12-^{2}H]$_{3}$-cortisone (d3E)(Andrew, et al. 2002). This approach has the advantage over use of the crude ratio of endogenous steroids where source pools of cortisol cannot be distinguished. Furthermore the commonly used ratio of endogenous steroids reflects a balance of reductase and dehydrogenase activities, where dehydrogenation can be catalysed by both 11βHSD1 and the type 2 isozyme, 11βHSD2 (Anderson, et al. 2021; Hughes, et al. 2012). Using tracer kinetics, Cobice et al (Cobice et al. 2017) showed the unique role of 11βHSD1 to form d3F using global 11βHSD1 knockout mice, who were unable to recycle active glucocorticoid from the d4F tracer. Additionally, H6PDH has received attention in determining the reaction direction of 11βHSD1, but its contribution and relative tissue contribution have not been quantified through tracer kinetics.

The measurement across the liver by arterio-venous sampling of production rates of d3F regenerated by 11βHSD1 (Andrew, et al. 2005; Basu, et al. 2006; Basu, et al. 2009) supports the view that, in humans, the majority of circulating cortisol arising from 11βHSD1-mediated glucocorticoid regeneration derives from the hepatic enzyme. Measurable production of cortisol generated by 11βHSD1, albeit at much slower rates, has also been quantified across adipose tissue and skeletal muscle (Hughes, et al. 2013), but not across human brain (Kilgour, et al. 2015) or heart (Iqbal, et al. 2014). These dynamic findings are consistent with the higher expression of 11βHSD1 in liver than in other tissues, and strongly suggests that hepatic 11βHSD1 exerts the biggest (non-adrenal) influence on the active and inactive glucocorticoids substrate and product in the circulation. Indeed transgenic over-expression of 11βHSD1 in the liver can correct the hypothalamic-pituitary-adrenal axis (HPA) phenotype of global 11βHSD1 deficiency (Paterson, et al. 2007). Here we tested the hypothesis that reduced hepatic 11βHSD1 reductase activity will decrease the proportion of the circulating

pool of cortisol derived through reduction of inert keto-steroids, and also reduce exposure of the brain and adipose tissue to regenerated active glucocorticoid. This is of relevance in understanding the consequences of tissue-specific up/down regulation of the enzyme and also design of the pharmacodynamic profiles of potential inhibitors.

MATERIALS AND METHODS

Materials

[9,11,12,12-^{2}H]$_4$-Cortisol (d4F), [9,12,12-^{2}H]$_3$-cortisol (d3F) and corticosterone were from Cambridge Isotopes, MA, USA. For LC-MS/MS, [9,11,12,12-^{2}H]$_4$-cortisol (certified reference material) was from Cerilliant (Round Rock, Texas, US), [2,2,4,6,6,9,12,12-^{2}H]$_8$-cortisone (d8E) from Sigma Aldrich (Poole, Dorset, UK) and [2,2,4,6,6,7,21,21-^{2}H]$_8$-corticosterone (d8B) from CK Isotopes, (Unthank, Leicestershire)). Solvents (methanol, acetonitrile and water) were glass-distilled HPLC and LC-MS grades (Fisher Scientific, Leicestershire, UK). α-Cyano-4-hydroxy cinnamic acid (CHCA), trifluoracetic acid, ammonium fluoride (NH_4F) and all other chemicals were from Sigma-Aldrich unless stated. Room temperature (RT) was 18-21ºC.

Animal Models and Husbandry

Male mice (*mus musculus*) were studied aged 9-12 weeks, congenic on a C57Bl/6J genetic background; *Hsd11b1*$^{f/f}$ mice, with *LoxP* sites flanking exon 3 of the *Hsd11b1* gene, were generated by Taconic Artemis (Cologne, Germany) (Verma, et al. 2018). *Hsd11b1*^{LKO} (LKO) mice, with hepatocyte 11βHSD1 deficiency, previously described with 94-100% knockdown (Zou, et al. 2018), were generated by crossing *Alb-Cre* transgenic mice with *Hsd11b1*$^{f/f}$ mice. *Hsd11b1*^{AKO} (AKO) mice, with adipocyte 11βHSD1 deficiency were generated by crossing *aP2-Cre* transgenic mice (He, et al. 2003) with *Hsd11b1*$^{f/f}$ mice. Experimental *Hsd11b1*^{LKO} or *Hsd11b1*^{AKO} mice were the offspring of male *Hsd11b1*^{LKO} mice or male *Hsd11b1*^{AKO} mice, respectively, each bred with female *Hsd11b1*$^{f/f}$ mice. Controls were *Hsd11b1*$^{f/f}$ littermates. Knockdown of *Hsd11b1* was achieved in adipose tissue in the AKO colony compared to control littermates and is demonstrated in Supplementary Figure 1 (~87% knockdown in

subcutaneous, ~73% in epidydimal and ~50% in mesenteric adipose tissues). Mice lacking *H6pdh* (generated using homologous recombination in embryonic stem cells to replace exons 2 and 3 with a neomycin resistance cassette (Lavery et al. 2006; Lavery, et al. 2008)) and their wild-type controls on a C57BL/6J background were generated in the University of Birmingham by heterozygous breeding and transferred to Edinburgh at the age of 3 months, under supervision of the Named Veterinary Surgeons at the Universities of Birmingham and Edinburgh. C57Bl/6J mice (Harlan Olac, Bicester, UK) were used to assess parameters for infusion to achieve steady state. Weights of animals are given in Supplementary Table 1. Studies were refined to be conducted in male mice only to permit comparison of multiple genotypes within practical experimental constraints.

In vivo Experimental protocols

All experiments on animals were carried out in accordance with the UK Home Office Animals (Scientific Procedures) Act of 1986 and European Directive 2010/63/EU, following approval by the University of Edinburgh Animal Welfare and Ethical Review Body and the Named Veterinary Surgeon. LKO and AKO genotypes were assigned by *Cre* positivity/negativity as described (Zou et al. 2018) and by PCR of tail biopsy as described previously (Lavery et al. 2006).

Mice were group housed (2-5 per cage) under controlled conditions: 12 h light/dark cycle at 21ºC with free access to standard rodent chow and water. Except for *H6pdh*$^{-/-}$ mice and their controls, mice were housed in standard cages. *H6pdh*$^{-/-}$ mice and their controls were housed in independently ventilated isolators for one week prior to experimentation due to transfer between facilities. Mice (n=3-6/group; exact group sizes indicated within legends) were infused with d4F (1.75 mg/day), at a rate of 1.03 µL/h by sub-cutaneous osmotic mini-pumps

(ALZET model 1003D or 1007D, Cupertino, CA, USA; vehicle dimethylsulfoxide: propylene glycol (50:50)), primed as per manufacturer's instructions and surgically implanted dorsally under isoflurane anesthesia with veterinary approved aseptic technique. Buprenorphine analgesia was administered peri-operatively, and mice allowed to recover in individual warm boxes for ~60 minutes before being returned to their home cages in groups. Post-operative welfare-related assessments were carried out under veterinary guidance for the duration of the infusion period. To assess timing to achieve steady state C57Bl/6J mice were euthanised by decapitation after infusion intervals of 24 h, 48 h or 7 days, with a further group receiving vehicle until 7 days. Genetically modified lines were similarly culled for comparison with their respective controls after infusion for 48 h. Plasma was prepared from trunk blood (collected in EDTA coated tubes) and tissues (liver, brain and adipose tissue) snap-frozen in liquid nitrogen and stored at -80^{o}C.

Quantitation of plasma and tissue steroids

The analyst was blinded to genotype. Steroids were quantified in plasma by liquid chromatography tandem mass spectrometry (LC-MS/MS) as described by Cobice et al (Cobice et al. 2017). Tissue steroids were assessed by MS using two analytical approaches, matrix assisted laser desorption ionisation (MALDI-MS) and LC-MS/MS. Methods previously reported for analysis of tissue steroids by Cobice et al (Cobice et al. 2017) were refined to reduce ion suppression, improve the limit of quantitation and thus allow detection of tracers in adipose tissue.

Analysis of corticosteroids in tissue extracts by LC-MS/MS

Snap-frozen adipose tissue (50-70 mg) was homogenised in acetonitrile + 0.1% formic acid (500 μL) using a bead homogeniser (Bead Ruptor Elite, Omni International, US, 1 cycle of

20 sec at 4 m/s maximum speed) and enriched with internal standards (1 ng; d8E and d8B). A calibration curve of analytes was prepared alongside the samples covering amounts in the range 0.0025–10 ng. Samples were subject to centrifugation (6,000 g, 5 min, 4 °C) and the supernatant (500 µL) spun down through centrifugal tube filter (0.22 µm SpinX Nylon; 13,000 g, 10 min, 4 °C). Samples and standards were transferred to an ISOLUTE® PLD+ 96-well plate cartridge (Biotage, Uppsala, Sweden) and elution performed under positive pressure (~15 psi, 10 min), and the eluate reduced to dryness under oxygen free nitrogen (OFN, 40 °C). The samples were dissolved in mobile phase (water:methanol, 70:30; 100 µL) shaken for 5-10 mins on an orbital plate shaker (250 rpm) and sealed before LC-MS/MS analysis using a Nexera 2 MP uHPLC system (Shimadzu, Kyoto, Japan) coupled to a QTRAP® 6500+ (SCIEX, Warrington, UK) equipped with a Turbospray interface in electrospray ionisation mode and operated with Analyst software v1.6.3. Separation was achieved on a Kinetex® C18 column (150 x 2.1mm, 1.7 µm, Phenomenex, Macclesfield, UK). Mobile phase (water (A) and methanol (B) each containing 0.05 mM NH_4F) were used at a flow rate of 0.3 mL/min, with an initial hold of 3 min at 50% B followed by a linear gradient to 100% B over 10 min and then re-equilibration to initial conditions (2 min). Column and auto-sampler temperatures were 50˚C and 10˚C respectively. Data were acquired by multiple reaction monitoring (collision energy, declustering potential, cell exit potential) of protonated molecular ions: d4F *m*/*z* 367→121 (29, 80, 16V); d3F *m*/*z* 366→121 (25, 121, 20V); d3E *m*/*z* 364→164 (31, 166, 14V); d8E *m*/*z* 369→169 (33, 96, 20V); corticosterone *m*/*z* 347→121 (29, 76, 8 V) and d8B *m*/*z* 355→125 (31, 56, 8V) with retention times of 2.8, 2.85 and 2.9 mins for d3F, d4F and F, 3.4 and 3.5 mins for d8E and d3E and 5.3 and 5.35 mins for d8B and corticosterone, respectively. Peak area ratios of steroid to corresponding isotopically labelled internal standard analogues were calculated and compared with corresponding calibration standards to generate a ng/g of tissue value.

240

241 ***Analysis of corticosteroids in tissue extracts by MALDI-MS***

242 Liver (~60 mg), adipose tissue (~100 mg) or half brain (sagittal, without pituitary, ~200 mg)
243 were mechanically homogenised in methanol-water (3 mL; 70:20 v/v), enriched with internal
244 standard, d8B (10 ng). Homogenates were shaken (15 min, RT) followed by centrifugation
245 (4000 g, 45 min, 4ºC). Supernatants of liver and adipose tissue and half of the brain extract
246 were reduced to dryness under OFN (RT; 40^0C) in Reacti-vials. Residues were reconstituted
247 in Girard T reagent (GirT; 100 µL, 5 mg/mL in methanol with 0.2% v/v trifluoroacetic acid)
248 and incubated (40 ^{0}C, 60 min), allowed to cool to RT and reduced to dryness under OFN. For
249 MALDI-FT-ICR-MS analysis, CHCA (200 µL, 10 mg/mL in 6:4 acetonitrile:water + 0.2%
250 v/v TFA) was added, vortexed and spotted (1 µL) on a MALDI stainless steel plate, allowed
251 to dry and stored under vacuum until analysis.

252

253 Tracer enrichment was assessed using a 12T SolariX MALDI-Fourier transform ion
254 cyclotron resonance-MS (Bruker Daltonics, MA, US) employing a Smart beam 1 kHz laser
255 and operated with SolariX control v1.5.0 (build 42.8). All analyses were carried out using
256 1000 laser shots and 1000 Hz laser frequency in positive ion mode. Laser power was
257 optimised at the outset and then fixed for all experiments. Laser focus was set to minimum
258 (99.7%) and 150 µm areas of spotted sample (1 µL) on Bruker MTP targets steel plate were
259 ionised by random walk. An average of 10 spectra within *m/z* 150-3000 was acquired using
260 continuous accumulation of selected ions (CASI^{TM}) mode to increase the signal-to-noise of
261 the ions with an isolation window at *m/z* 458 ± 50 Da and collected with a 4 Mword time-
262 domain transient to resolve all peaks. The GirT derivatives of d4F (d4F-GirT), d3F (d3F-
263 GirT) and d3E (d3E-GirT), corticosterone-GirT and d8B (d8B-GirT), were monitored at *m/z*,
264 480.3370, 479.3307, 477.3151, 460.3166 and 468.3672 respectively. Spectral

characterisation of steroids was assessed using a standard mix (100 pg, methanol: water (1:1)) of d4F and d3F spotted onto the same MALDI plate. Accurate masses were aligned with individual spectra (Bruker Compass Data Analysis software v4.1), and a single-point calibration against the abundance of d8B-GirT ion applied.

Data and Statistical Analysis

For tissue homogenates, the average intensities of the d4F-GirT, d3E-GirT, d3F-GirT and d8B-GirT ions are presented as ratios of derivatives of d4F/d8B, d3E/d8B, d3F/d8B, d4F/d3F and corticosterone/d8B. The Gir T derivatives of labelled cortisol and cortisone yield very similar intensities upon quantitation by MALDI, and thus the ratio of abundances of the derivatives of the tracer steroids to internal standard was used for relative quantitation. The amount of internal standard (d8B) was normalised per mg tissue. Concentrations of steroids measured by LC-MS/MS were quantified against linear calibration curves of peak area ratios of analytes versus internal standards, prepared concomitantly and accepted with a regression coefficient, $r>0.99$. For quadrupole analyses, the intensities of deuterated steroids were corrected for the contributions of isotopologues with naturally occurring ^{13}C and deuterium, assessed using reference standards; these species could be distinguished spectrally using FT-ICR-MS. Amounts of steroids in tissues were expressed as a ratio to internal standard and corrected to 100 mg tissue.

Unless otherwise stated, data are expressed as mean±standard error of the mean and differences were analysed using a one-way ANOVA with Fisher's post-test, Kruskal Wallis with mean rank tests or Mann Whitney U as appropriate (Statistica, Tibco, Palo Alto, USA). Statistical significance was set at $p<0.05$. Breeding of LKO and AKO mice was planned to achieve group sizes of a minimum of n=5, allowing assessment of a 50% change of

11βHSD1 activity measured by d4F/d3F ratio to be detected in brain with a power of 90% (p=0.05) (Cobice et al. 2017). The effect of disruption of *H6pdh* was assessed in groups of n=3.

RESULTS

Tracer Turnover in Tissues: Timing of Measurements

Following tracer infusions for 24 h, 48 h, or 7 days, concentrations of tracers in plasma and amounts in tissues were compared (Fig 1). Tracers were not detected in plasma or tissue of mice receiving vehicle infusion, providing reassurance of lack of interfering analytical signals. In plasma, the concentrations of d4F decreased between 24 and 48 h and then the mean value stabilised, but with more variability between animals at 7 days (Fig 1A). Similar to plasma, d4F concentrations in all tissues were highest at 24 h, stabilising between 48 h and 7 days with greater inter-individual variability at 7 days than at earlier times (Fig 1B). Of the tissues tested, the highest amounts of d4F were found in liver at all time points, being ~10-fold higher than in adipose tissue and ~12-fold higher than in brain after 7 days infusion. D4F was undetectable in adipose tissue at 24 h but became detectable at the later time points. Endogenous corticosterone was detectable in plasma of control mice but not following infusion. The amounts of corticosterone reduced to around 5% of control levels in liver and brain by the 24 h time point and was undetectable by 7 days. In the case of adipose tissue, corticosterone abundance declined on average to ~51% (Range 44-70%) of control amounts by 24 h, 31% (Range 15-44%) by 48 h and remained around this level until 7 days (Range 18-55%).

D3E was detected but could not be quantified in plasma due to lack of a commercial analytical standard. Similar to d4F, d3F concentrations declined in plasma after 24 h, remained stable between 48 h and 7 days, and showed greater inter-individual variability at 7 days than at earlier times (Fig 1D). D3E and d3F were detected in liver and brain at 24 h but were undetectable in adipose tissue at this time point (Figs 1C and D). Amounts of both d3E

and d3F were higher in liver than in other tissues and reduced after 24 h. Levels of both d3E and d3F remained stable in adipose tissue and brain from 48 h to 7 days and their abundances in adipose tissue ultimately exceeded those of brain by 7 days.

Turnover of d4F to d3F as an indicator of 11βHSD1 activity was assessed as the d4F/d3F ratio the value of which is reduced with greater 11-keto reduction. The mean value of d4F/d3F ratio remained relatively stable during the 48 h to 7 day period in plasma, but again there was more variability between animals at the later time (Fig 1F). The d4F/d3F ratio was lower in all tissues than in plasma at all time points and was similar in brain and liver (Fig 1G). The d4F/d3F ratio took longer to equilibrate in adipose tissue, achieving a lower ratio than in other tissues by Day 7, but again was variable at this time point. Due to lower inter-individual variability, and having reached steady-state, 48 h was chosen as the most robust timepoint to compare mice of differing genotypes. In all subsequent experiments, findings in respective control mice were similar to those in the C57BL/6J mice.

INFLUENCE OF H6PDH ON REGENERATION OF D3F FROM D3E

Given that H6PDH is important for 11βHSD1 reductase activity and thus generation of d3F from d4F (via d3E), we asked whether *H6pdh*$^{-/-}$ mice could generate d3F to any degree and if so, were all tissues influenced similarly. Data are shown in Figure 2. D4F was detected in similar concentrations in plasma of *H6pdh*$^{-/-}$ mice and their littermate controls (Fig 2A). Regenerated d3F was detected in the circulation of both genotypes (Fig 2D), but the d4F/d3F ratio was approximately 6 fold higher in the plasma of *H6pdh*$^{-/-}$ mice compared to their controls (Fig 2F). This extrapolated into whole body rates of appearance of d3F that were approximately 6-fold lower in *H6pdh*$^{-/-}$ mice than control, 0.05±0.002 vs 0.33±0.039 mg/day, respectively. These findings are consistent with 11βHSD1 reductase activity (driven by

H6PDH) as a major but not exclusive contributor to plasma and tissue glucocorticoid regeneration. Moreover, the d4F/d3F ratio in the plasma of *H6pdh*$^{-/-}$ mice was higher than in either of the mouse lines with tissue-specific disruption of 11βHSD1; in hepatocytes (Fig 3F) or adipose tissue (Fig 4F). Similarly in liver, d3F levels were lower in *H6pdh*$^{-/-}$ mice, compared with controls (Fig 2E) and the d4F/d3F ratio was higher overall in liver and brain in *H6pdh*$^{-/-}$ mice compared to controls (Fig 3G). It was not possible to calculate a ratio for adipose tissue because d3F was not detected in that tissue in *H6pdh*$^{-/-}$ mice.

STEROID TURNOVER IN PLASMA AND TISSUES IN MICE WITH HEPATOCYTE-SPECIFIC DISRUPTION OF 11bHSD1

To investigate how hepatic 11βHSD1 contributes to the amounts of regenerated active steroid in the circulating pool as well as in liver, brain and adipose tissue, d3F was measured, comparing LKO mice to their respective controls following d4F infusion. Data are shown in Figure 3. The concentrations of d4F and d3F in the circulation of LKO mice were unchanged compared with their littermate wild-type controls (Figs 3A, 3D), and consequently the d4F/d3F ratio was unchanged (Fig 3F). These data equate to whole body rates of appearance of d3F of 0.20±0.03 vs 0.26±0.03 mg/day in LKO vs control respectively. Amounts of d4F were higher (Fig 3B) and those of d3F lower (Fig 3E) in liver of LKO mice compared to control littermates, without differences in adipose tissue and brain. In contrast to plasma, within the liver of in LKO mice the d4F/d3F ratio was higher (Fig 3G) compared to littermate controls, again without any change in adipose tissue or brain. These data suggest that 11βHSD1 in liver makes a negligible contribution to circulating levels of active glucocorticoids in mice but is important for the intra-hepatic balance of active and inert glucocorticoids.

STEROID TURNOVER IN PLASMA AND TISSUES IN MICE WITH DISRUPTION OF 11B-HSD1 IN ADIPOSE TISSUE

Similarly the contribution of 11βHSD1 in adipose tissue to circulating and tissue pools of regenerated glucocorticoids was studied, comparing AKO mice to their respective controls. Data are shown in Figure 4. The concentration of d4F in the circulation of AKO mice was unchanged compared with littermate controls (Fig 4A), whereas those of d3F were lower in AKO mice (Fig 4D). Accordingly, the ratio of d4F/d3F in plasma was higher in AKO mice than in littermate controls (Fig 4F), revealing lower whole body rates of appearance of d3F in AKO mice (0.15±0.02 vs 0.35±0.08 mg/day; AKO vs WT respectively). Moreover, the rate of appearance of d3F in plasma in the AKO mice was lower than that in LKO mice, but remained higher than in *H6pdh*$^{-/-}$ mice (each Mann Whitney U Test, $p<0.05$). The d4F/d3F ratio was higher in all tissues of the AKO mice compared with their littermate controls (Fig 4G).

DISCUSSION AND CONCLUSIONS

Hepatocyte-mediated glucocorticoid regeneration *in vivo* in male mice affected exposure to regenerated steroids only within the liver and not the circulation or measured tissues (adipose tissue or brain). This was not anticipated given that studies in humans show comparable rates of appearance of glucocorticoids across the liver to whole body appearance measured in the circulation (Andrew et al. 2005; Basu et al. 2006; Basu et al. 2009). In contrast, disruption of 11βHSD1 expression in adipose tissue reduced levels of regenerated steroid in blood, liver and brain as well as in adipose tissue. Lastly it was shown that H6PDH plays a significant, but not exclusive, role in glucocorticoid regeneration in liver, brain and adipose tissue.

Overall the regeneration of active glucocorticoid by 11βHSD1 measured using the d4F tracer in the mouse models was representative of previous results in humans, except steady state took longer to achieve in mice, around 48 h versus 3 h in humans, which may reflect differences between sub-cutaneous and intravenous infusion (Andrew et al. 2002). The temporal pattern of tracer appearance in the liver resembled that of plasma and in both cases the data became more variable between mice at 7 days. The reason for this was not investigated further, but may have related to more variable delivery by the pumps towards the end of their operation, albeit they were designed to work for 1 week. The intermediate, d3E, and regenerated d3F stabilised by 48 h in blood and liver but at lower levels than d4F. The lower levels of d4F and d3F in brain compared with other tissues may reflect the active export of cortisol via the ABCB1 transporter. This transporter, which actively exports cortisol (Nixon, et al. 2016) and, by inference, d4F and d3F, is expressed in brain. However it is worth noting that tissues such as brain may have specific sub-regions of high expression of

11βHSD1, such as cerebellum and hippocampus (Holmes, et al. 2010; Moisan, et al. 1990), and greater regeneration of d3F in these regions may be diluted within whole tissue measures.

While fluctuations in circulating glucocorticoid levels are rapidly reflected in the hepatic pool of steroids, adipose tissue pool appears buffered in humans (Hughes et al. 2013) and responds in hours/days, reflecting longer-term, sustained changes in prevailing glucocorticoids. Plausibly this slow turnover might protect adipose tissue from intermittent and short-lasting surges of cortisol in the blood. Methodological improvements allowed detection of tracer in adipose tissue, which had not been achieved in previous studies (Cobice et al. 2017) allowing the slower achievement of steady state in adipose tissue than in brain or liver in mouse to be quantified. Endogenous corticosterone was also washed out of adipose tissue more slowly than other tissues. It is assumed that steroids enter cells by passive diffusion due to their lipophilic nature and are sequestered in lipid droplets in adipose tissue. The slow turnover of the adipose tissue pool, typical of lipophilic molecules (Bruno, et al. 2021), may be due to constrained efflux of steroids from the triglyceride-rich lipid droplets, whereas efflux from the more phospholipid-rich environment of the brain could be more rapid.

The contribution of 11βHSD1 in all tissues was evident through greater dilution of d4F with d3F (approximately three-fold) compared with plasma (measured as d4F/d3F ratio). Even in the absence of H6PDH, residual d3F generation could still be seen with lower d4F/d3F ratios in tissues than in blood. Previously the d4F tracer had been administered to mice with global disruption of 11βHSD1 and d3F was not generated, indicative of 11βHSD1 being the sole enzymatic route of reduction of d3E to d3F. Here, the finding of small but residual regeneration of d3F in mice lacking H6PDH suggests that H6PDH is the main, but possibly not the not sole, driver of 11β-reduction. The remaining 11β-reduction may be driven through an alternative

source of co-factor, such as glucose-6-phosphate dehydrogenase (G6PDH); indeed patients with glycogen storage disease with perturbations in the G6PDH cycle do show disturbances in their HPA phenotypes (Rossi, et al. 2020). The change in co-factor balance from predominantly NADPH towards NAPD in mice lacking H6PDH would be anticipated to alter the equilibrium of 11βHSD1 in favour of dehydrogenation (Lavery et al. 2006). This may have manifest in lower circulating concentrations of d4F under infusion conditions (as an indicator of increased clearance, including dehydrogenation). D4F concentrations in plasma were not significantly different in *H6pdh-/-* mice compared to their wild-type controls, however, this must be viewed with caution as group sizes were small and not designed to test such questions.

In mice with disruption of 11βHSD1 in either hepatocyte or adipose tissue, regeneration of d3F was attenuated in the tissue targeted by the genetic disruption, with altered 11-keto-reduction of tracer detected most sensitively through changes in the local d4F/d3F ratio. The circulating concentrations of d4F were not different between genotypes, and thus other clearance pathways, such as by 11βHSD2, appeared unaffected. The d4F/d3F ratio more than doubled within liver following hepatocyte disruption compared to around a 50% increase in the ratio in adipose tissue following adipocyte disruption in keeping with greater abundance of the enzyme in liver than adipose tissue (Chapman et al. 2013). The 2-fold reduction in the amount of d3F in livers of the LKO mice compared to littermate controls suggests that under steady-state conditions roughly half of the active glucocorticoid within the liver derives from hepatic regeneration via 11βHSD1. The remaining d3F in liver is likely to be delivered from the blood, although it remains possible that non-hepatocyte cells may contribute to regeneration of hepatic d3F. Indeed Kupffer cells and vasculature both express 11βHSD1 and may contribute locally, though to a limited degree given >94% knockdown in hepatic *Hsd11b1* mRNA levels in LKO mice, compared to littermate controls (Zou et al. 2018)).

It was striking that the increase in the ratio of d4F/d3F in liver was not evident in the circulation in LKO mice. It is possible that d3F regenerated from d3E within liver is routed through further irreversible metabolism, such as by A-ring reduction and conjugation, which might be studied in the future through urine or faecal collection. Alternatively, it may be actively transported into the bile rather than re-entering the circulation; glucocorticoids are excreted into the bile in rodents (albeit reports relate to endogenous corticosterone and not exogenous cortisol) (Morris 2015). Therefore, in rodents cortisol regenerated by 11βHSD1 in liver may act in liver but not beyond, but it should be noted the route of biliary excretion of glucocorticoids does not translate to humans (Morris 2015). These findings of restrained effects within the liver align with the subtle systemic metabolic phenotype of mice lacking 11βHSD1 in liver. However it should be noted that these mice did have enlarged adrenal glands (Lavery, et al. 2012), suggesting endocrine effects originating from the hepatic deficiency of 11βHSD1. Moreover, transgenic over-expression of 11βHSD1 in liver rescued the HPA axis phenotype of the global knockout mouse (Paterson et al. 2007). The HPA responses in this setting have been shown to be strain specific (Carter, et al. 2009) thus this finding, and how it translates to humans, merits further exploration.

In contrast, adipocyte-specific disruption of 11βHSD1 changed the d4F/d3F ratio not only in adipose tissue but also in the blood, and remote tissues, liver and brain. This may be of pathological relevance in obesity which is associated with an increase in adipose tissue 11βHSD1 expression in humans (Rask, et al. 2001; Rask, et al. 2002), potentially modifying glucocorticoid action systemically. However, an important caveat is that *Ap2-Cre*, used to generate AKO mice, is expressed in cell types other than adipocytes, including macrophages, endothelial cells and certain regions of the brain (Jeffery, et al. 2014; Lee, et al. 2013;

McInnes, et al. 2012). Such ectopic expression may contribute to the phenotype, though this is unlikely to be of sufficient magnitude to explain the global effect observed (Lee et al. 2013). Moreover Christy et al showed that *Hsd11b1* was not expressed in the endothelial cells of blood vessels of male mice, being located instead in the smooth muscle (Christy, et al. 2003).

The strengths of this study lie in the use of tracer kinetics which can distinguish sources of steroids, coupled with analysis by gold standard mass spectrometry, as opposed to less specific immunoassay which still dominates the preclinical literature. A unique set of genetic modifications have allowed dissection of the roles of the different tissues, with caveats discussed over the specificity of the *aP2-Cre*, which might be overcome by alternative Cre driver e.g. adiponectin-Cre. Future opportunities exist using MALDI imaging to measure the distribution of the tracers within specific brain regions (Cobice et al. 2017). Only gonadal adipose tissues from young, male mice were studied with a view to comparing key tissues, however the nature of different adipose tissue depots differ. Further studies in both sexes are required, particularly given the differences in distribution of adipose tissue between sexes, as well as sexual dimorphism in enzyme activity (Jamieson, et al. 2000) and other regulatory factors such as binding globulins (Toews, et al. 2021) in rodents. It would also be valuable to study animal under dietary high-fat challenge or over-expressing *Hsd11b1* in metabolic tissues, for example simulating the up-regulation of enzyme expression in adipose tissue which occurs in human obesity in both sexes (Rask et al. 2001; Rask et al. 2002). Further glucocorticoid-target tissues may be of interest for similar studies including skeletal muscle and bone and investigation of whether kinetics of turnover change in pathophysiological states such as insulin resistance and obesity and models with genetic disruption of *hsd11b1* in populations of brain cells would provide valuable insight. Lastly care must be taken when

extrapolating data to humans, although mouse models have proven helpful in the development of 11βHSD1 inhibitors,

In summary, the active glucocorticoid generated by hepatic 11βHSD1is largely constrained to the liver in mice, whereas the steroid pool in adipose tissue undergoes slower turnover and drains active glucocorticoid into the circulation where it reaches other tissues through endocrine delivery. Thus inhibitors which access 11βHSD1 in adipose tissue may have broader reaching effects compared with those just targeting the liver, including attenuation of glucocorticoid action in brain.

Conflicts of Interest

SPW, JRS and BRW are academic inventors on patents relating to 11β-hydroxysteroid dehydrogenase 1 inhibitors, owned by the University of Edinburgh and licensed to Actinogen Medical Ltd. SPW, JRS, RA and BRW are consultants to Actinogen Medical Ltd.

Funding: The work was supported by British Heart Foundation (RG-05-00 8; 2011) and its Centre for Research Excellence (BHF RE/08/001; 2008-date), and the Wellcome Trust (WT083184, 2008; 107049/Z/15/Z; 2016). BRW is a Wellcome Trust Senior Investigator.

Acknowledgements: We are grateful for technical assistance from Val Kelly and the staff at the Biomedical Research Facility and the analytical chemists of Edinburgh Clinical Research Facility Mass Spectrometry Core Laboratory and SIRCAMS. For the purpose of open access, the author has applied a Creative Commons Attribution (CC BY) licence to any Author Accepted Manuscript version arising from this submission

FIGURE LEGENDS

FIGURE 1: Tracer kinetics after timed infusions in mice

9,11,12,12-[$^2H_4$]-Cortisol (d4F) was infused for 24 h, 48 h or 7 days into male C56BL6J mice (n=3-6) by minipump. Steroids were quantified in blood (absolute concentrations) and tissues (liver, brain, gonadal adipose tissue; ratios versus d8-corticosterone (d8B; internal standard) respectively; d4F (A) and (B), d3E (C), d3F (D) and (E). D4F/d3F ratios are presented in plasma (F) and tissues (G). Individual data points are shown with mean and standard error of the mean superimposed and compared in plasma by Mann-Whitney U tests and in tissues by one-way ANOVA (with Fisher's post-hoc test) at matched timepoints. * $p<0.05$. ND= Not detected.

FIGURE 2: Tracer kinetics after timed infusions in mice with whole body disruption of hexose-6-phosphate dehydrogenase

9,11,12,12-[$^2H_4$]-Cortisol (d4F) was infused by minipump for 48 h into male mice (n=3/genotype) with whole body disruption of hexose-6-phosphate dehydrogenase (KO) and their littermate controls (C). Steroids were quantified in blood (absolute concentrations) and tissues (liver, brain, gonadal adipose tissue; ratios versus d8-corticosterone (d8B; internal standard) respectively; d4F (A) and (B), d3E (C), d3F (D) and (E). d4F/d3F ratios are presented in plasma (F) and tissues (G). Individual data points were compared in plasma by Mann-Whitney U tests and in tissues by Kruskal Wallis ANOVA (with mean rank post-hoc test). * $p<0.05$. ND = Not detected

FIGURE 3: Tracer kinetics after timed infusions in mice with hepatocyte-specific disruption of 11β-hydroxysteroid dehydrogenase type 1

9,11,12,12-[$^2H_4$]-Cortisol (d4F) was infused for 48 h into male mice with hepatocyte specific-disruption of 11β-hydroxysteroid dehydrogenase type 1 (LKO; n=5) and their floxed littermate controls (C; n=5) by minipump. Steroids were quantified in blood (absolute concentrations) and tissues (liver, brain, gonadal adipose tissue; ratios versus d8-corticosterone (d8B; internal standard) respectively; d4F (A) and (B), d3E (C), d3F (D) and (E). D4F/d3F ratios are presented in plasma (F) and tissues (G). Individual data points are shown with mean and standard error of the mean superimposed and compared in plasma by Student's *t* tests and in tissues by two-way ANOVA (with Fisher's post-hoc tests). * $p<0.05$, ** $p<0.01$*** $p<0.001$. G= Genotype, T= Tissue.

FIGURE 4: Tracer linetics after timed infusions in mice with adipocyte-specific disruption of 11β-hydroxysteroid dehydrogenase type 1

9,11,12,12-[$^2H_4$]-Cortisol (d4F) was infused for 48 h into male mice with adipocyte specific-disruption of 11β-hydroxysteroid dehydrogenase type 1 (AKO, n=5) and their floxed littermate controls (C, n=5) by minipump. Steroids were quantified in blood (absolute concentrations) and tissues (liver, brain, gonadal adipose tissue; ratios versus d8-corticosterone (d8B; internal standard) respectively; d4F (A) and (B), d3E (C), d3F (D) and (E). D4F/d3F ratios are presented in plasma (F) and tissues (G). Individual data points are shown with mean and standard error of the mean superimposed and compared in plasma by Student's *t* tests and in tissues by two-way ANOVA (with Fisher's post-hoc tests). * $p<0.05$, *** $p<0.001$. Trends are indicated if $p<0.1$.

Supplementary Figure 1

Transcripts of *Hsd11b1* was substantially reduced in adipose tissue beds from mice adipocyte specific-disruption of 11β-hydroxysteroid dehydrogenase 1 (AKO) versus their floxed littermate controls (WT). Data are measurements by real-time PCR of abundance of mRNAs encoding 11β-HSD1 normalised to that of a house-keeping genes (TATA binding protein (TBP)) in subcutaneous, gonadal and mesenteric adipose tissue of WT and AKO mice (n=8 and 5 respectively) Primer-probe sets for *Hsd11b1* and *Tbp* (Mm00476182_m1 and Mm00446973_m1, respectively) were purchased from Applied Biosystems. AU (arbitrary units).

REFERENCES

Ajjan RA, Hensor EMA, Del Galdo F, Shams K, Abbas A, Fairclough RJ, Webber L, Pegg L, Freeman A, Taylor AE, et al. 2022 Oral 11β-HSD1 inhibitor AZD4017 improves wound healing and skin integrity in adults with type 2 diabetes mellitus: a pilot randomized controlled trial *European Journal of Endocrinology* **186** 441.

Anderson AJ & Walker BR 2013 11beta-HSD1 inhibitors for the treatment of type 2 diabetes and cardiovascular disease. *Drugs* **73** 1385-1393.

Anderson AJ, Andrew R, Homer NZM, Hughes KA, Boyle LD, Nixon M, Karpe F, Stimson RH & Walker BR 2021 Effects of obesity and insulin on tissue-specific recycling between cortisol and cortisone in men. *Journal of Clinical Endocrinology and Metabolism* **106** e1206-e1220.

Andrew R, Smith K, Jones GC & Walker BR 2002 Distinguishing the activities of 11b-hydroxysteroid dehydrogenases *in vivo* using isotopically labelled cortisol. *Journal of Clinical Endocrinology & Metabolism* **87** 277-285.

Andrew R, Westerbacka J, Wahren J, Yki-Jarvinen H & Walker BR 2005 The contribution of visceral adipose tissue to splanchnic cortisol production in healthy humans. *Diabetes* **54** 1364-1370.

Andrews RC, Rooyackers O & Walker BR 2002 Effects of the 11beta-hydroxysteroid dehydrogenase inhibitor carbenoxolone on insulin sensitivity in men with type 2 diabetes. *Journal of Clinical Endocrinology & Metabolism* **88** 285-291.

Basu R, Edgerton DS, Singh RJ, A. C & Rizza RA 2006 Splanchnic cortisol production in dogs occurs primarily in the liver: Evidence for substantial hepatic specific 11beta hydroxysteroid dehydrogenase type 1 activity. *Diabetes* **55** 3013-3019.

611 Basu R, Basu A, Grudzien M, Jung P, P. J, M J, Singh RJ, M S & Rizza RA 2009 Liver is the
612 site of splanchnic cortisol production in obese nondiabetic humans. *Diabetes* **58** 39-45.
613 Bruno CD, Harmatz JS, Duan SX, Zhang Q, Chow CR & Greenblatt DJ 2021 Effect of
614 lipophilicity on drug distribution and elimination: Influence of obesity. *Birtish Journal of*
615 *Clinical Pharmacology* **87** 3197-3205.
616 Carter RN, Paterson JM, Tworowska U, Stenvers DJ, Mullins JJ, Seckl JR & Holmes MC
617 2009 Hypothalamic-pituitary-adrenal axis abnormalities in response to deletion of 11beta-
618 HSD1 is strain-dependent. *Journal of Neuroscience* **21** 879-887.
619 Chapman K, Holmes MC & JR S 2013 11β-Hydroxysteroid Dehydrogenases: Intracellular
620 Gate-Keepers of Tissue Glucocorticoid Action. *Physiological Reviews* **93** 1139-1206.
621 Christy C, Hadoke PWF, Paterson JM, Mullins JJ, Seckl JR & Walker BR 2003
622 Glucocorticoid action in mouse aorta; localisation of 11b-hydroxysteroid dehydrogenase type
623 2 and effects on responses to glucocorticoids in vitro. *Hypertension* **42** 580-587.
624 Cobice DF, Livingstone DEW, McBride A, MacKay CL, Walker BR, Webster SP & Andrew
625 R 2017 Quantification of 11β-hydroxysteroid dehydrogenase 1 kinetics and
626 pharmacodynamic effects of inhibitors in brain using mass spectrometry imaging and stable-
627 isotope tracers in mice. *Biochemical Pharmacology* **148** 88-99.
628 Feig PU, Shah S, Hermanowski-Vosatka A, Plotkin D, Springer MS, Donahue S, Thach S,
629 Klein EJ, Lai E & Kaufman KD 2011 Effects of an 11β-hydroxysteroid dehydrogenase type 1
630 inhibitor, MK-0916, in patients with type 2 diabetes mellitus and metabolic syndrome.
631 *Diabete Obes Metab* **13** 498-504.
632 He W, Barak Y, Hevener A, Olson P, Liao D, Le J, Nelson M, Ong E, Olefsky JM & Evans
633 RM 2003 Adipose-specific peroxisome proliferator-activated receptor γ knockout causes
634 insulin resistance in fat and liver but not in muscle. *Proceedings of the National Academy of*
635 *Sciences USA* **100** 15712-15717.

636 Heise T, Morrow L, Hompesch M, Häring H-U, Kapitza C, Abt M, Ramsauer M, Magnone
637 M-C & Fuerst-Recktenwald S 2014 Safety, efficacy and weight effect of two 11β-HSD1
638 inhibitors in metformin-treated patients with type 2 diabetes. *Diabetes, Obesity and*
639 *Metabolism* **16** 1070-1077.
640 Hermanowski-Vosatka A, Balkovec JM, Cheng K, Chen HY, Hernandez M, Koo GC, Le
641 Grand CB, Li Z, Metzger JM, Mundt SS, et al. 2005 11b-HSD1 inhibition ameliorates
642 metabolic syndrome and prevents progression of atherosclerosis in mice. *The Journal of*
643 *Experimental Medicine* **202** 517-527.
644 Holmes MC, Carter RC, Noble J, Chitnis S, Dutia A, Paterson JM, Mullins JJ, Seckl JR &
645 Yau JLW 2010 11beta-hydroxysteroid dehydrogenase type 1 expression is increased in the
646 aged mouse hippocampus and parietal cortex and causes memory impairments. *The Journal*
647 *of Neuroscience* **30** 6916-6920.
648 Hughes KA, Webster SP & Walker BR 2008 11-Beta-hydroxysteroid dehydrogenase type 1
649 (11beta-HSD1) inhibitors in type 2 diabetes mellitus and obesity. *Expert Opinion in*
650 *Investigative Drugs* **17** 481-496.
651 Hughes KA, Reynolds RM, Critchley HO, Andrew R & Walker BR 2013 Glucocorticoids
652 turn over slowly in human adipose tissue. *Journal of Clinical Endocrinology & Metabolism*
653 **95** 4696-4702.
654 Hughes KA, Manolopoulos KN, Iqbal J, Cruden NL, Stimson RH, Reynolds RM, Newby
655 DE, R A, Karpe F & Walker BR 2012 Recycling between cortisol and cortisone in human
656 splanchnic, subcutaneous adipose and skeletal muscle tissues *in vivo. Diabetes* **61** 1357-1364.
657 Iqbal J, R A, Cruden NL, CJ K, Hughes KA, Newby DE, Hadoke PWF & Walker BR 2014
658 The misnomer of 'aldosterone receptor antagonists': cortisol not aldosterone occupies
659 mineralocorticoid receptors in human heart. *Journal of Clinical Endocrinology & Metabolism*
660 **99** 915-922.

661 Jamieson PM, Walker BR, Chapman KE, Rossiter S & Seckl JR 2000 11b-Hydroxysteroid
662 dehydrogenase type 1 is a predominant 11b-reductase in intact perfused rat liver. *J.*
663 *Endocrinol* **165** 685-692.
664 Jeffery E, Berry R, Church CD, Yu s, Shook BA, Horsley V, Rosen ED & Rodeheffer MS
665 2014 Characterization of Cre recombinase models for the study of adipose tissue. *Adipocyte* **3**
666 206-211.
667 Katz DA, Liu W, Locke C, Jacobson PB, Barnes DM, Basu R, An G, Rieser MJ, Daszkowski
668 D, Groves F, et al. 2013 Peripheral and central nervous system inhibition of 11β-
669 hydroxysteroid dehydrogenase type 1 in man by the novel inhibitor, ABT-384. *Transl*
670 *Psychiatry* **3** e295.
671 Kilgour AHM, Semple S, Marshall I, Andrews PC, Andrew R & Walker BR 2015 11b-
672 Hydroxysteroid dehydrogenase activity in brain does not contribute to systemic
673 interconversion of cortisol and cortisone in healthy men. *Journal of Clinical Endocrinology*
674 *& Metabolism* **100** 483-489.
675 Kotelevtsev Y, Holmes MC, Burchell A, Houston PM, Schmoll D, Jamieson P, Best R,
676 Brown R, Edwards CR, Seckl JR, et al. 1997 11beta-hydroxysteroid dehydrogenase type 1
677 knockout mice show attenuated glucocorticoid-inducible responses and resist hyperglycemia
678 on obesity or stress. *Proceedings of the National Academy of Sciences of the United States of*
679 *America* **94** 14924-14929.
680 Lavery GG, Walker EA, Draper N, Jeyasuria P, Marcos J, Shackleton CHL, Parker KL,
681 White PC & Stewart PM 2006 Hexose-6-phosphate dehydrogenase knock-out mice lack 11b-
682 hydroxysteroid dehydrogenase type 1-mediated glucocorticoid generation. *Journal of*
683 *Biological Chemistry* **281** 6546-6551.
684 Lavery GG, Walker EA, Turan N, Rogoff D, Ryder JW, Shelton JM, Richardson JA, Falciani
685 F, White PC, Stewart PM, et al. 2008 Deletion of hexose-6-phosphate dehydrogenase

686 activates the unfolded protein response pathway and induces skeletal myopathy. *Journal of*
687 *Biological Chemistry* **283** 8453-8461.
688 Lavery GG, Zielinska AE, Gathercole LL, Hughes BA, Semonjous N, Guest P, Saqib K,
689 Sherlock M, Reynolds G, Morgan SA, et al. 2012 Lack of significant metabolic abnormalities
690 in mice with liver-specific disruption of 11b-hydroxysteroid dehydrogenase type 1.
691 *Endocrinology* **153** 3236–3248.
692 Lee KY, Russell SJ, Ussar S, Boucher J, Vernochet C, Mori MA, Smyth G, Rourk M,
693 Cederquist C, Rosen ER, et al. 2013 Lessons on conditional gene targeting in mouse adipose
694 tissue. *Diabetes* **62** 864-874.
695 Liu J, Wang L, Zhang A, Di W, Zhang X, Wu L, Yu J, Zha J, Lv S, Cheng P, et al. 2011
696 Adipose-tissue targeted 11b-hydroxysteroid dehydrogenase type 1 inhibitor protects against
697 diet-induced obesity. *Endocrine Journal* **58** 199-209.
698 McInnes KJ, Smith LB, N.I. H, Saunders PTK, Andrew R & Walker BR 2012 Deletion of the
699 Androgen Receptor in adipose tissue in male mice elevates Retinol Binding Protein 4 and
700 reveals independent effects on visceral fat mass and on glucose homeostasis. *Diabetes* **61**
701 1072–1081.
702 Moisan M-P, Seckl JR & Edwards CRW 1990 11b-Hydroxysteroid dehydrogenase
703 bioactivity and messenger RNA expression in rat forebrain: localization in hypothalamus,
704 hippocampus and cortex. *Endocrinology* **127** 1450-1455.
705 Montaron MF, Drapeau E, Dupret D, Kitchener P, Aurousseau C, Le Moal M, Piazza PV &
706 Abrous DN 2006 Lifelong corticosterone level determines age-related decline in
707 neurogenesis and memory *Neurobiology of Aging* **27** 645-654.
708 Morris D 2015 Why do humans have two glucocorticoids: A question of intestinal fortitude
709 *Steroids* **102** 32-38.

Morton NM, Paterson JM, Masuzaki H, Holmes MC, Staels B, Fievet C, Walker BR, Flier JS, Mullins JJ & Seckl JR 2004 Novel adipose tissue-mediated resistance to diet-induced visceral obesity in 11beta-hydroxysteroid dehydrogenase type 1-deficient mice. *Diabetes* **53** 931-938.

Mylonas KJ, Turner NA, Bageghni SA, Kenyon CJ, White CI, McGregor K, Kimmitt RA, Sulston R, Kelly V, Walker BR, et al. 2017 11β-HSD1 suppresses cardiac fibroblast CXCL2, CXCL5 and neutrophil recruitment to the heart post MI *Journal of Endocrinology* **233** 315-327.

Nixon M, Mackenzie SD, Taylor AI, Homer NZM, Livingstone DEW, Mouras R, Morgan RA, Mole DJ, Stimson RH, Reynolds RM, et al. 2016 ABCC1 confers tissue-specific sensitivity to cortisol versus corticosterone: a rationale for safer glucocorticoid replacement therapy *Science Translational Medicine* **8** 352ra109.

Paterson JM, Holmes MC, Kenyon CJ, Carter R, Mullins JJ & Seckl JR 2007 Liver-selective transgene rescue of hypothalamic-pituitary-adrenal axis dysfunction in 11beta-hydroxysteroid dehydrogenase type 1-deficient mice. *Endocrinology* **148** 961-966.

Rask E, Olsson T, Söderberg S, Andrew R, Livingstone DEW, Johnson O & Walker BR 2001 Tissue-specific dysregulation of cortisol metabolism in human obesity. *Journal of Clinical Endocrinology & Metabolism* **86** 1418-1421.

Rask E, Walker BR, Söderberg S, Livingstone DEW, Eliasson M, Johnson O, Andrew R & Olsson T 2002 Tissue-specific changes in peripheral cortisol metabolism in obese women: increased adipose 11b-hydroxysteroid dehydrogenase type 1 activity. *Journal of Clinical Endocrinology & Metabolism* **87** 3330-3336.

Rosenstock J, Banarer S, Fonseca VA, Inzucchi SE, Sun W, Yao W, Hollis G, Flores R, Levy R, Williams WV, et al. 2010 The 11-Beta-hydroxysteroid dehydrogenase type 1 inhibitor

734 INCB13739 improves hyperglycemia in patients with Type 2 diabetes inadequately
735 controlled by metformin monotherapy. *Diabetes Care* **33** 1516-1522.
736 Rossi A, Simeoli C, Salerno M, Ferrigno R, Della Casa R, Colao A, Strisciuglio P, Parenti G,
737 Pivonello R & Melis D 2020 Imbalanced cortisol concentrations in glycogen storage disease
738 type I: evidence for a possible link between endocrine regulation and metabolic derangement
739 *Orphanet Journal fo Rare Diseases* **15** 99.
740 Sandeep TC, Andrew R, Homer NZM, Andrews RC, Smith K & Walker BR 2005 Increased
741 *in vivo* regeneration of cortisol in adipose tissue in human obesity and effects of the 11b-
742 hydroxysteroid dehydrogenase type 1 inhibitor carbenoxolone. *Diabetes* **54** 872-879.
743 Shah S, Hermanowski-Vosatka A, Gibson k, Ruck RA, Jia G, Zhang J, Hwang PM, Ryan
744 NW, Langdon RB & Feig PU 2011 Efficacy and safety of the selective 11β-HSD-1 inhibitors
745 MK-0736 and MK-0916 in overweight and obese patients with hypertension. . *J Am Soc*
746 *Hypertension* **5** 166.
747 Sooy K, Webster SP, Noble J, Binnie M, Walker BR, Seckl JR & Yau JLW 2010 Partial
748 deficiency or short-term inhibition of 11beta-hydroxysteroid dehydrogenase type 1 improves
749 cognitive function in aging mice. *Journal of Neuroscience* **30** 13867-13872.
750 Sooy K, J N, McBride A, Binnie M, Yau JL, Walker BR & Webster SP 2015 Cognitive and
751 disease-modifying effects of 11β-hydroxysteroid dehydrogenase type 1 inhibition in male
752 Tg2576 Mice, a model of Alzheimer's Disease. *Endocrinology* **156** 4592-4603.
753 Toews JNC, Hammond GL & Viau V 2021 Liver at the nexus of rat postnatal HPA axis
754 maturation and sexual dimorphism. *Journal of Endocrinology* **248** R1-R17.
755 Verma M, Kipari T, Zhang Z, Man T, NZ H, JR S, Holmes MC & Chapman KE 2018 11β-
756 hydroxysteroid dehydrogenase-1 deficiency alters brain energy metabolism in acute systemic
757 inflammation. *Brain, Behaviour and Immunity* **69** 223-234.

758 Webster SP, Ward P, Binnie M, Craigie E, McConnell KM, Sooy K, Vinter A, Seckl JR &
759 Walker BR 2007 Discovery and biological evaluation of adamantyl amide 11beta-HSD1
760 inhibitors. *Bioorganic and Medicinal Chemistry Letters* **17** 2838-2843.
761 Webster SP, McBride A, Binnie M, Sooy K, Andrew R, Pallin T, Hunt H, Perrior T, Ruffles
762 V, Ketelbey J, et al. 2016 Selection and early clinical evaluation of the brain-penetrant 11β-
763 hydroxysteroid dehydrogenase type 1 (11β-HSD1) inhibitor UE2343 (Xanamem®). *British*
764 *Journal of Pharmacology* **174** 396-408.
765 Yau JL, Noble J & Seckl JR 2011 11beta-hydroxysteroid dehydrogenase type 1 deficiency
766 prevents memory deficits with aging by switching from glucocorticoid receptor to
767 mineralocorticoid receptor-mediated cognitive control. *Journal of Neuroscience* **31** 4188-
768 4193.
769 Yau JL, Wheelan N, Noble J, Walker BR, Webster SP, Kenyon CJ & JR S 2015
770 Intrahippocampal glucocorticoids generated by 11β-HSD1 affect memory in aged mice.
771 *Neurobiology of Aging* **36** 334-343.
772 Yau JL, McNair KM, Noble J, Brownstein D, Hibberd C, Morton N, Mullins JJ, Morris RG,
773 Cobb S & Seckl JR 2007a Enhanced hippocampal long-term potentiation and spatial learning
774 in aged 11beta-hydroxysteroid dehydrogenase type 1 knock-out mice. *J Neurosci* **27** 10487-
775 10496.
776 Yau JLW, Noble J, Kotelevtsev Y, Hibberd C, Mullins JJ & Seckl JR 2001 Lack of tissue
777 glucocorticoid reactivation in 11beta-hydroxysteroid dehydrogenase type 1 knockout mice
778 ameliorates age-related learning impairments. *Proceedings of the National Academy of*
779 *Sciences of the United States of America* **98** 4716-4721.
780 Yau JLW, McNair KM, Noble J, Brownstein D, Hibberd C, Morton NM, Mullins JJ, Morris
781 RG, Cobb S & Seckl JR 2007b Enhanced hippocampal long-term potentiation and spatial

782 learning in aged 11b-hydroxysteroid dehydrogenase type 1 knock-out mice. *Journal of*
783 *Neuroscience* **27** 10487-10496.
784 Zou X, Ramachandran P, Kendall TJ, Pellicoro A, Dora E, Aucott R, Manwani K, Man TY,
785 Chapman KE, Henderson NC, et al. 2018 11Beta-hydroxysteroid dehydrogenase-1 deficiency
786 or inhibition enhances hepatic myofibroblast activation in murine liver fibrosis. *Hepatology*
787 **doi: 10.1002/hep.29734**.
788

Khan et al Figure 1

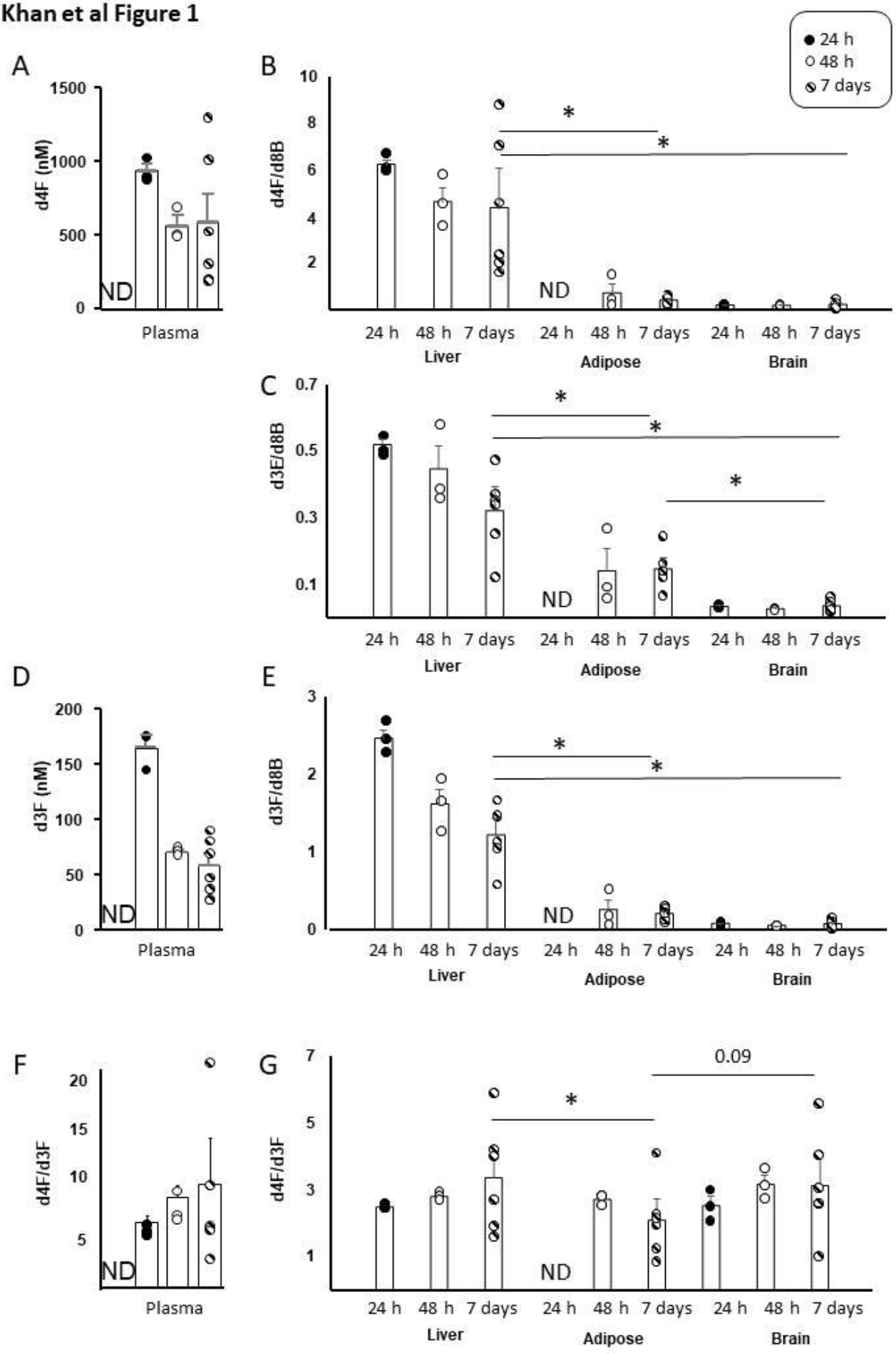

Khan et al Figure 2

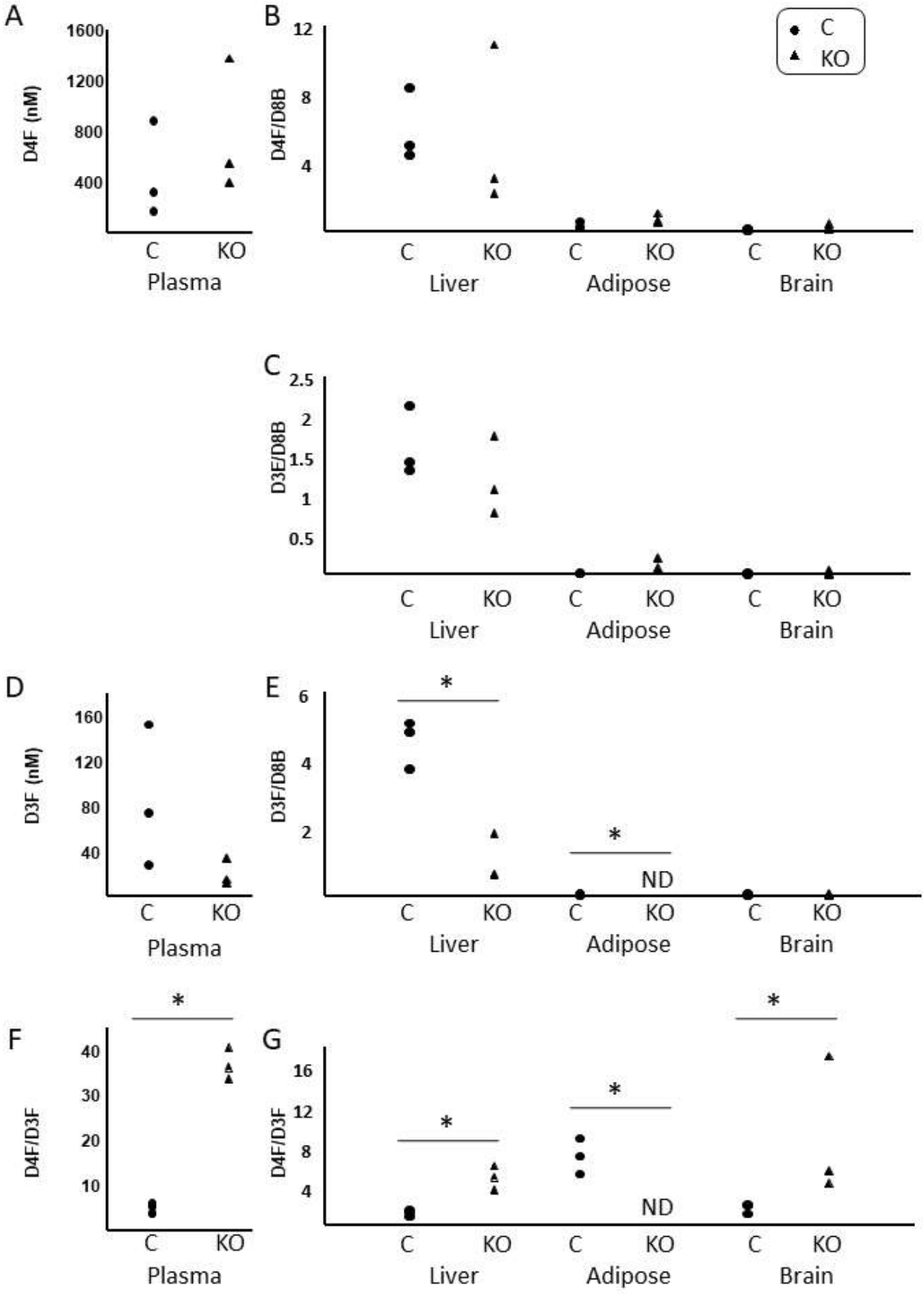

Khan et al Figure 3

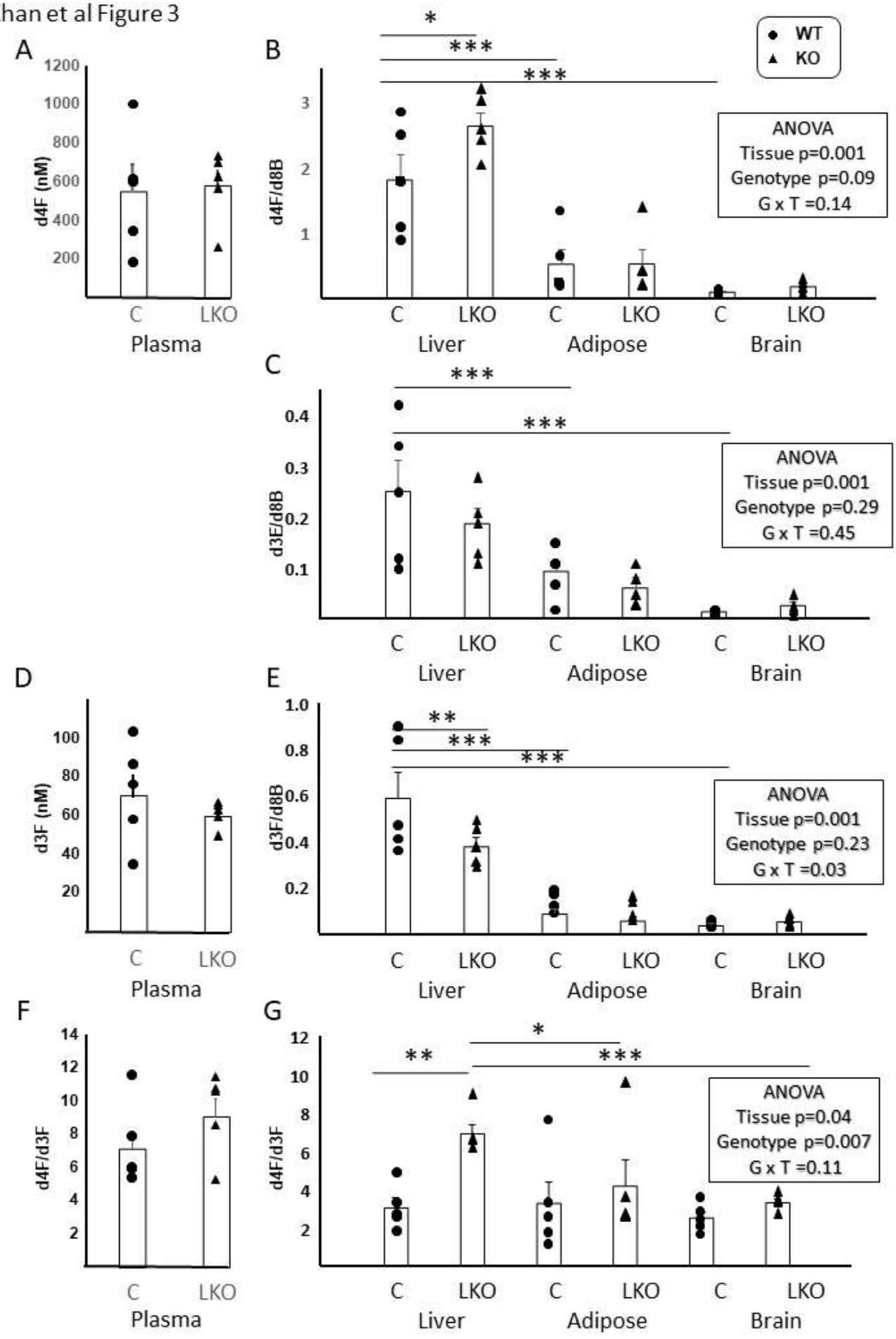

Khan et al Figure 4

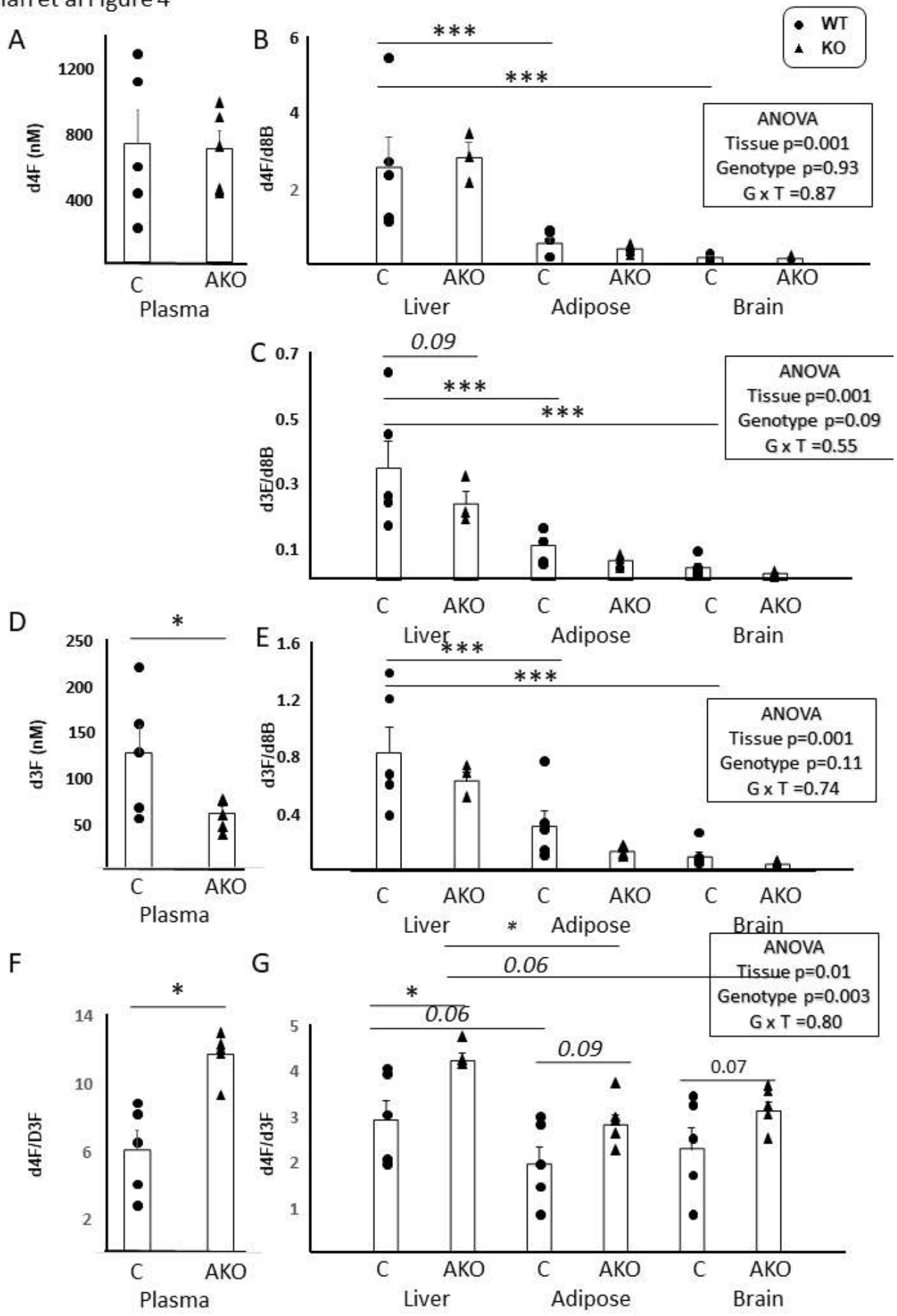

Khan et al Supplementary Figure 1